

Ionothermal Route to Layered Two-Dimensional Polymer-Frameworks Based on Heptazine Linkers

Michael J. Bojdys,^{*,†} Stephanie A. Wohlgemuth,[†] Arne Thomas,[‡] and Markus Antonietti[†]

[†]Max Planck Institute of Colloids and Interfaces, Department of Colloid Chemistry, Research Campus Golm, 14476 Potsdam, Germany, and [‡]Technische Universität Berlin, Funktionsmaterialien, Englische Strasse 20, 10587 Berlin, Germany

Received May 7, 2010; Revised Manuscript Received July 14, 2010

Introduction

Layered two-dimensional polymer-frameworks are fascinating research targets. The development of reliable synthetic routes to periodic, covalent molecular layers touches on structural, analytical, technological and theoretical aspects of the natural sciences and has a profound impact on fundamental research and its realization, as seen for example in graphene research¹ and the recent field of 2D and 3D covalent frameworks.^{2–6} The linking of organic molecules to long-range ordered moieties or materials is classically limited to noncovalent interactions,^{7–9} while covalent polymerization reactions usually only yield structurally randomized networks.^{10,11}

The most challenging hurdle in the synthesis of extended, yet precisely defined 2D and 3D structures based on covalent chemistry is widely believed to be the requirement, that the reaction linking individual organic constituents needs to be reversible, allowing the scaffold to arrange to the thermodynamic, well ordered product rather than the kinetic, amorphous structure.^{12,13} In addition, the design of the building blocks must allow for growth into a nonperturbed, regular geometry (i.e., at least three latent bond-forming sites enclosing an appropriate angle) and for sufficient chemical stability.

One such promising candidate for a condensation and bonding pattern of monomeric units was described first in 1834 by Justus von Liebig for the condensation of cyanamides to several amorphous C/N materials which he arbitrarily named melamine, melam, melem and melon, with increasing temperature of formation.¹⁴ Yet it was very much later that the “possible formation mechanisms of melem” were discussed.^{15,16} From literature, the formation of the heptazine unit proceeds under formal deamination of the partaking species, and under ideal conditions no excess of reactive molecules which would be available for side-reactions is created. Note further that the condensation process requires no more than a triazine and a carbonitrile group to proceed. Hence, a self-propagating condensation mechanism employing a single molecular precursor which contains both the triazine- and the carbonitrile-functionality at its termini can be used (cf. Figure 1). Since the reaction is performed in a closed system under constant temperature all steps in the condensation process remain essentially reversible.

The nature of the group R chosen as a linker between the triazine- and the carbonitrile-functionality (as seen in Figure 1) is accessible to the synthetic chemist. The compounds used are bisubstituted aromatics, preferably with two cyano-groups in *para* positions. One of the nitriles can then be converted into a

triazine group (an ammeline derivative) with dicyandiamide (DCDA) in a base catalyzed reaction. The formation of the stable, aromatic triazine unit drives the reaction to completion. The aromatic carbonitriles with one triazine-functionality readily precipitate from boiling 2-propanol after short reaction times (cf. Experimental Section). Such a designed molecular precursor is ready to undergo the thermal condensation outlined above, and the particular 3-fold symmetry and planar arrangement of the trisubstituted heptazine unit then allows the synthesis of planar, 2D frameworks which are expected to stack in a graphitic fashion (cf. Figure 1).

However, the formation of Liebig’s melem in this thermally induced condensation reaction was reported to be at around 370 and 390 °C, which was verified by a differential scanning calorimetry study on the condensation of cyanamide (cf. Supporting Information).^{15–17} This discards all standard solvents. Kanatzidis and co-workers have previously pointed out the limited choice of appropriate media for synthetic applications at intermediate temperatures (i.e., 150–350 °C) and successfully applied alkali-metal polysulfide melts in the synthesis of low-dimensional ternary chalcogenides.¹⁸ The eutectic mixture of lithium and potassium halides (e.g., LiCl/KCl 45:55 wt %, $T_m = 352$ °C, or LiBr/KBr 52:48 wt %, $T_m = 348$ °C)¹⁹ has been known for some time as a medium for electrochemical processes, in particular in high-temperature galvanic cells²⁰ and more recently as a solvent for salts of lanthanides and actinides.²¹ Sundermeyer et al. showed already in the 1960s that known organic chemistry can be performed in molten salts.^{22,23} Among the successfully synthesized compounds were carbonyl and fluorocarbonyl pseudohalogenides²⁴ as well as cyanides, cyanates and thiocyanates of both silicon and carbon.²⁵ In this context, Sundermeyer explicitly points out the good solvating properties of the eutectic mixture of LiCl and KCl with respect to nitrides, carbides, cyanides, cyanates, and thiocyanates, and we have previously used the LiCl/KCl eutectic as a solvent in the synthesis of a crystalline, graphitic carbon nitride species.⁴ For our means the LiBr/KBr eutectic was identified as a good solvent due to its high-temperature stability and a melting point below the polycondensation point of *s*-heptazine. From laboratory experience, it was given preference over the chloride analogue due to its superior solvation properties for the small molecular precursors employed in the synthesis and subsequent aggregates of higher molecular weight.

In the work at hand, we report the synthesis of three molecular building blocks based on 1,4-aryl, 4,4'-biphenyl and 1,3-aryl each containing a triazine and a carbonitrile functionality and the thermally induced autocondensation of these into three respective heptazine-based, ordered, 2D, layered polymer frameworks (HBFs) in an eutectic salt melt of lithium and potassium bromide

*Corresponding author. Telephone: +49 331 567 9569. E-mail: m.j.bojdys.02@cantab.net.

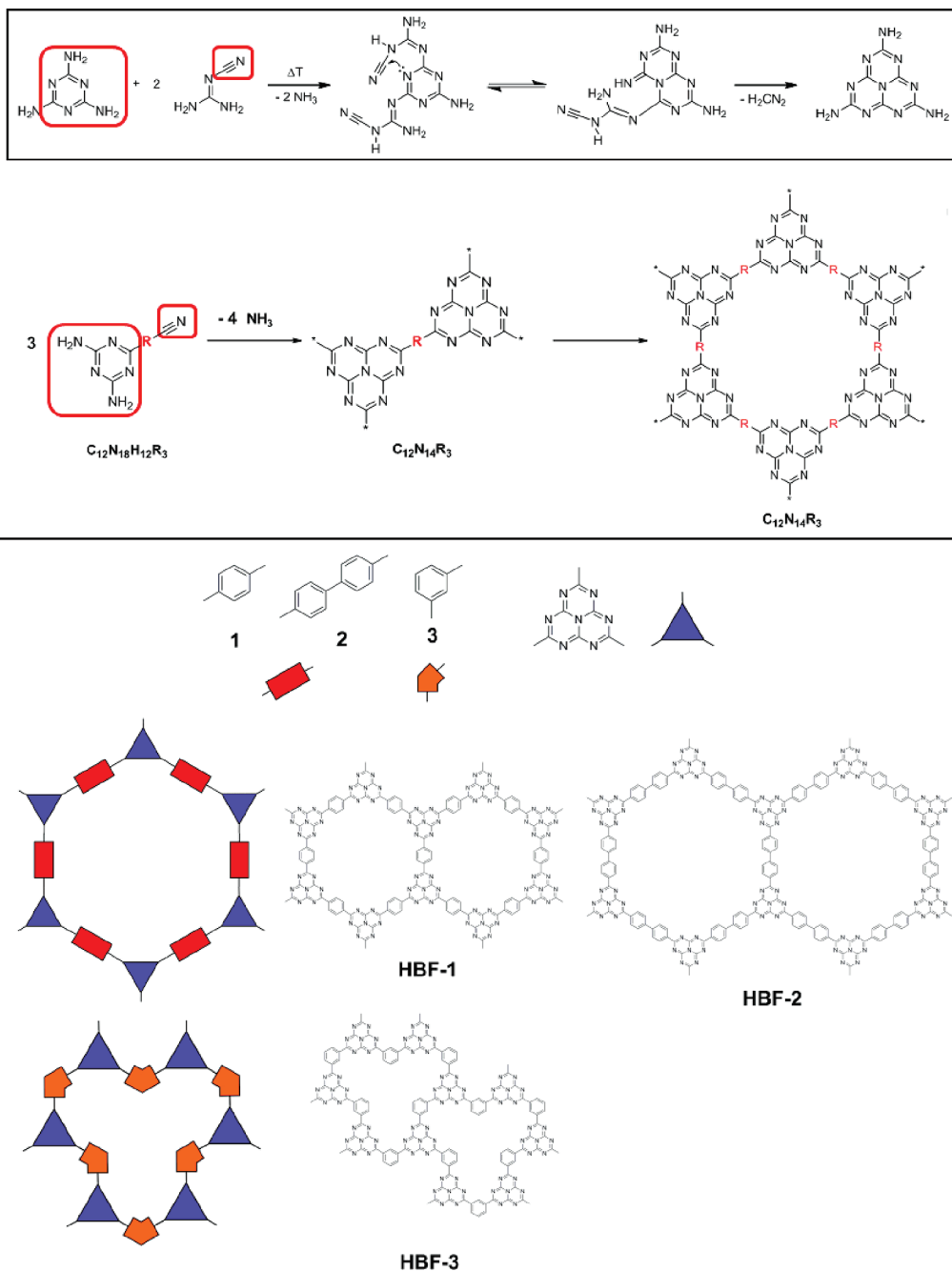


Figure 1. (Upper part, boxed) Proposed reaction mechanism for the condensation of melem.^{15,16} (Upper part) Formal condensation mechanism of a monomer containing a triazine- and carbonitrile functionality to a heptazine based framework. (Lower part) Condensation motifs of 2D heptazine-based frameworks (HBFs). The heptazine linker is shown as a planar triangle (blue) and the aromatic spacer as a coplanar rectangle (red), with **1**, **2**, and **3** being constituents of the precursors ArCNTz, BiPhCNTz and 1,3-ArCNTz and of the frameworks **HBF-1**, **HBF-2**, and **HBF-3**, respectively.

as solvent of choice. We thereby show that by making use of heptazine-chemistry, the toolbox of the synthetic chemist can be expanded to link organic building blocks entirely by strong covalent bonds and to give not only chemically and thermally stable, but also well-ordered, lightweight materials.

Experimental Section

Synthesis of 4-(4,6-Diamino-1,3,5-triazin-2-yl)benzodicyanide (ArCNTz). 1,4-Dicyanobenzene (5.0 g, 38.2 mmol, 98%) and dicyandiamide (3.25 g, 38.2 mmol, 99%) were heated to 105 °C in 2-propanol (140 cm³). KOH (0.36 g, 6.4 mmol) was dissolved in 2-propanol (10 cm³) and added dropwise to the reaction mixture which was then refluxed at 105 °C for 1 h. The solution was poured into cold water and the white precipitate collected

and washed with cold water until neutral. After removal of the solvent and drying *in vacuo*, 4-(4,6-diamino-1,3,5-triazin-2-yl)benzodicyanide was obtained as a white powder. Yield: 7.50 g, 35.3 mmol, 92.4% for C₁₀H₈N₆. Anal. Calcd for C₁₀H₈N₆: C, 56.60; H, 3.80; N, 39.60. Found: C, 56.39; H, 3.79; N, 36.82. In addition, the compound was verified as pure by ¹H and ¹³C NMR (cf. Supporting Information).

Synthesis of HBF-1. A quartz ampule of the dimensions *l* = 120 mm, o.d. = 30 mm, i.d. = 27 mm was charged with 4-(4,6-diamino-1,3,5-triazin-2-yl)benzodicyanide (0.50 g, 2.4 mmol) and a mixture of lithium bromide and potassium bromide (3 g, 52:48 wt %) under inert atmosphere. The ampule was sealed under vacuum, heated and kept at the terminal temperature of 430 °C for 48 h. After cooling, the homogeneously brown-black block of salt and product was stirred for overnight in distilled water to

dissolve the salt, and was subsequently washed with water, THF and acetone to remove residual salt and poorly condensed residues. HBF-1 was obtained as a brown-black powder and dried *in vacuo* at 150 °C. Yield: 0.27 g, 0.47 mmol, 58.8% for C₃₀H₁₂N₁₄. Anal. Calcd for C₃₀H₁₂N₁₄: C, 63.38; H, 2.52; N, 34.49. Found: C, 57.84; H, 2.52; N, 33.81.

Synthesis of 4'-(4,6-Diamino-1,3,5-triazin-2-yl)biphenyl-4-carbonitrile (BiPhCNTz). 4,4'-Biphenyldicarbonitrile (3.0 g, 14.25 mmol, 97%) and dicyandiamide (1.21 g, 14.24 mmol, 99%) were heated to 110 °C in 2-propanol (100 cm³). KOH (0.13 g, 2.32 mmol) was dissolved in 2-propanol (10 cm³) and added dropwise to the reaction mixture which was then refluxed at 110 °C for 18 h. The solution was poured into cold water and the yellow precipitate collected and washed with cold water until neutral. After removal of the solvent and drying *in vacuo*, 4'-(4,6-diamino-1,3,5-triazin-2-yl)biphenyl-4-carbonitrile was obtained as a yellow powder. Yield: 3.86 g, 13.39 mmol, 94.0% for C₁₆H₁₂N₆. Anal. Calcd for C₁₆H₁₂N₆: C, 66.66; H, 4.20; N, 29.15. Found: C, 65.61; H, 4.27; N, 26.30. In addition, the compound was verified as pure by ¹H and ¹³C NMR (cf. Supporting Information).

Synthesis of HBF-2. A quartz ampule of the dimensions *l* = 120 mm, o.d. = 30 mm, i.d. = 27 mm was charged with 4'-(4,6-diamino-1,3,5-triazin-2-yl)biphenyl-4-carbonitrile (0.34 g, 1.18 mmol) and a mixture of lithium bromide and potassium bromide (5 g, 52:48 wt %) under inert atmosphere. The ampule was sealed under vacuum, heated and kept at the terminal temperature of 400 °C for 24 h. After cooling, the homogeneously black block of salt and product was stirred for overnight in distilled water to dissolve the salt, and was subsequently washed with water, THF and acetone to remove residual salt and poorly condensed residues. HBF-2 was obtained as a black powder and dried *in vacuo* at 150 °C. Yield: 0.23 g, 0.29 mmol, 74.6% for C₄₈H₂₄N₁₄. Anal. Calcd for C₄₈H₂₄N₁₄: C, 72.35; H, 3.04; N, 24.61. Found: C, 67.37; H, 3.56; N, 23.00.

Synthesis of 3-(4,6-Diamino-1,3,5-triazin-2-yl)benzonitrile (1,3-ArCNTz). 1,3-Dicyanobenzene (5.0 g, 38.2 mmol, 98%) and dicyandiamide (3.25 g, 38.2 mmol, 99%) were heated to 110 °C in 2-propanol (130 cm³). KOH (0.36 g, 6.4 mmol) was dissolved in 2-propanol (10 cm³) and added dropwise to the reaction mixture which was then refluxed at 110 °C for 12 h. The solution was poured into cold water and the white precipitate collected and washed with cold water until neutral. After removal of the solvent and drying *in vacuo*, 3-(4,6-diamino-1,3,5-triazin-2-yl)benzonitrile was obtained as a white powder. Yield: 7.82 g, 36.85 mmol, 96.5% for C₁₀H₈N₆. Anal. Calcd for C₁₀H₈N₆: C, 56.60; H, 3.80; N, 39.60. Found: C, 56.26; H, 3.86; N, 36.68. In addition, the compound was verified as pure by ¹H and ¹³C NMR (cf. Supporting Information).

Synthesis of HBF-3. A quartz ampule of the dimensions *l* = 120 mm, o.d. = 30 mm, i.d. = 27 mm was charged with 3-(4,6-diamino-1,3,5-triazin-2-yl)benzonitrile (0.50 g, 2.4 mmol) and a mixture of lithium bromide and potassium bromide (3 g, 52:48 wt %) under inert atmosphere. The ampule was sealed under vacuum, heated and kept at the terminal temperature of 400 °C for 48 h. After cooling, the homogeneously brown-black block of salt and product was stirred for overnight in distilled water to dissolve the salt, and was subsequently washed with water, THF and acetone to remove residual salt and poorly condensed residues. HBF-3 was obtained as a brown-black powder and dried *in vacuo* at 150 °C. Yield: 0.28 g, 0.49 mmol, 61.3% for C₃₀H₁₂N₁₄. Anal. Calcd for C₃₀H₁₂N₁₄: C, 63.38; H, 2.13; N, 34.49. Found: C, 57.62; H, 2.15; N, 31.72.

Results and Discussion

Elemental analysis of HBF-1, HBF-2, and HBF-3 gives the chemical formulas C_{30.0}N_{15.04}H_{17.5}, C_{48.0}N_{14.05}H_{30.2}, and C_{30.0}-N_{14.16}H_{13.3} which is in good correspondence to the theoretical values of C₃₀N₁₄H₁₂, C₄₈N₁₄H₂₄, and C₃₀N₁₄H₁₂, respectively.

The high nitrogen contents observed for the three networks discount a multitude of possible binding motifs which are not based on heptazine units—e.g., a binding motif based on triazine (C₃N₃) linkers, as seen for the covalent triazine frameworks CTF-1 and CTF-2,^{5,26} would imply lower nitrogen contents for each framework (i.e., nitrogen content for HBF-1 would be 21.86 wt % as to observed 33.81 wt %, for HBF-2 would be 12.27 wt % as to observed 23.00 wt %, and for HBF-3 would be 21.86 wt % as to observed 31.72 wt %). With thermogravimetric analysis yielding residual masses of approximately 1–1.5% at 900 °C under synthetic air for the three respective systems, it is highly unlikely that the inorganic components of the eutectic salt melt are regularly incorporated in the framework (cf. Supporting Information).

Extensively progressed condensation and the covalent linking of the frameworks by heptazine units were additionally probed by attenuated total reflection Fourier transform infrared (ATR FT-IR) and magic angle spinning nuclear magnetic resonance (MAS NMR) spectroscopy. Vibrational spectra of HBF-1, HBF-2 and HBF-3 showed that the broad ammonia bands at around 3200 cm⁻¹, indicative of secondary and primary amines (and their intermolecular hydrogen bonding) which are still present for the mono- and oligomeric building blocks at the start of the reaction and at lower temperatures, next to disappear for the high temperature condensation products. Since aromatic C–H bonds are an integral part of the aromatic linkers, some remaining bands in this region are expected. The carbonitrile bands around 2250 cm⁻¹ also gradually disappear as the condensation is driven to completion. The aromatic C–C band at 1600 cm⁻¹ remains visible throughout the process, which corroborates the results from elemental microanalysis that no aromatic groups are eliminated. The characteristic breathing mode of the triazine and heptazine units at 800 cm⁻¹ is also preserved throughout the process. Combined with the results of the elemental microanalysis, it is safe to assume that the material we are looking at consist of condensed domains at least on the nanometer scale with few terminal groups or defects (cf. Figure 2).

The solid-state ¹³C MAS NMR spectra for HBF-1, HBF-2, and HBF-3 are presented in Figure 3. The resonances observed at approximately 169 and 163 ppm for each framework are indicative of the two different carbon environments expected for a trisubstituted heptazine, with the former connected directly to the aryl linker and the latter forming the core of the heptazine unit. The resonances of the bridging aromatic linkers are situated between 140 and 120 ppm. The observed number of chemical environments corresponds to the expected number for heptazine-based frameworks and are in agreement with previous reports in literature for heptazine-based materials.^{27–30}

To assess the crystal structure of HBF-1, HBF-2, and HBF-3 the powder X-ray patterns of the best-ordered condensation products were chosen, namely the most thoroughly condensed products obtained at 430, 410, and 400 °C, respectively. The observed peak positions for HBF-1 generally give a good correlation with the calculated in-plane Bragg peak positions of hexagonal unit sheet with the parameters (cf. Supporting Information). The hexagonal unit cell is populated in the *a*–*b* plane with heptazine units bridged by phenylene linkers (cf. Figure 4) giving chemically sound bond lengths and angles. In this model unit cell the first low-angle peak is assigned to an in-plane reflection, yielding unit cell parameters of *a* = *b* = 18.590 Å. This is much larger than the unit cell parameters calculated and observed for the corresponding triazine (C₃N₃) bridged network (i.e., CTF-1, *a* = *b* = 14.547 Å)⁵ or for the isoelectronic borazine (B₃O₃) bridged network (i.e., COF-1, *a* = *b* = 15.420 Å)³¹ further supporting the formation of the larger heptazine unit in the frameworks. The packing motif of these sheets, however, is not trivial to deduce, although the principal packing peak at

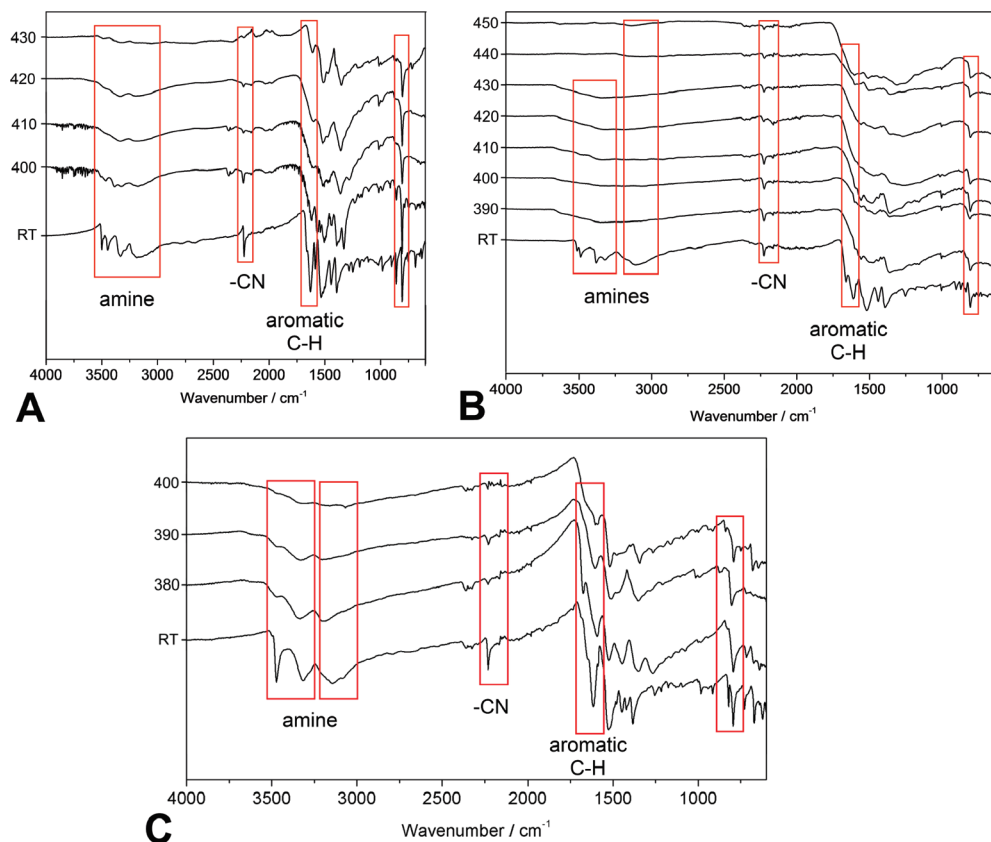


Figure 2. FTIR spectra of different condensation stages of HBF-1, HBF-2 and HBF-3 and their respective monomers (A, B, and C, respectively) in LiBr/KBr melt at varying temperatures.

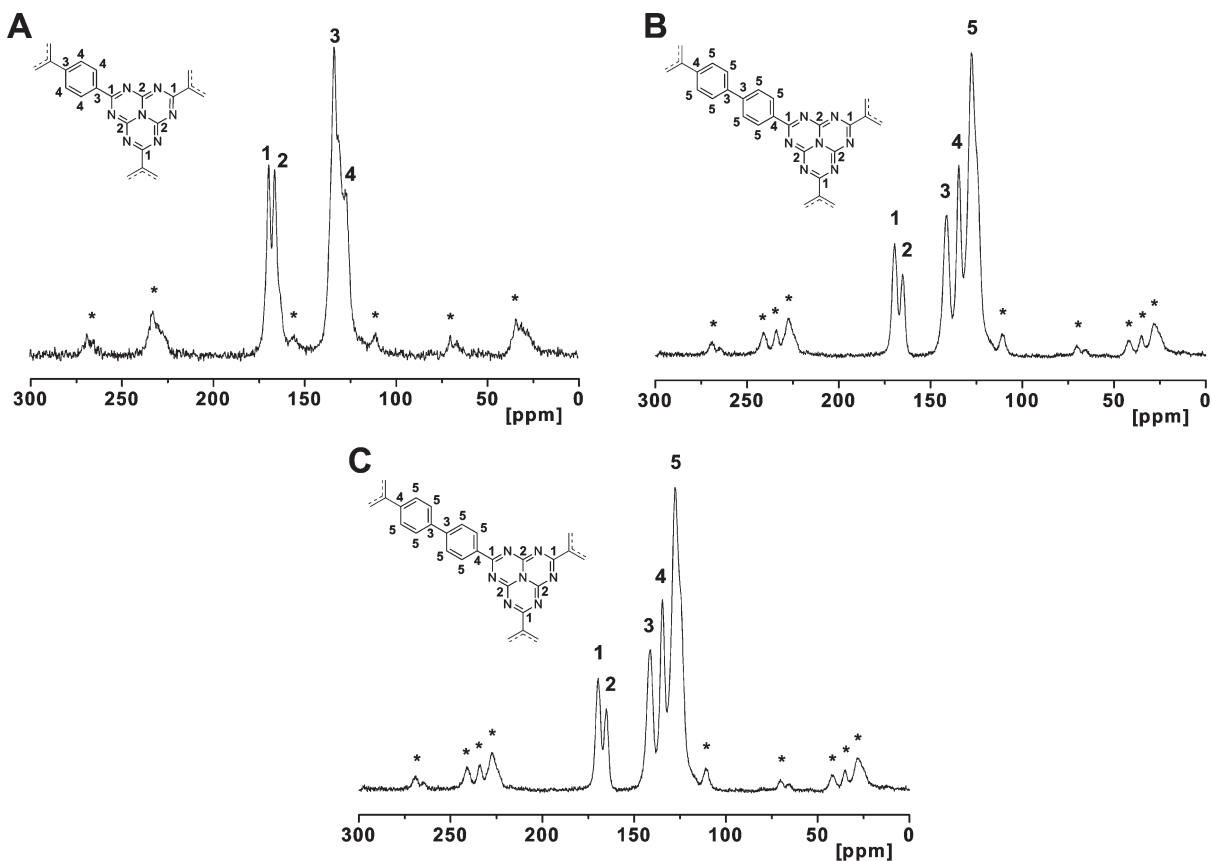


Figure 3. ^{13}C MAS NMR spectra of (A) HBF-1, (B) HBF-2, and (C) HBF-3 with indicated spinning sidebands (* in black).

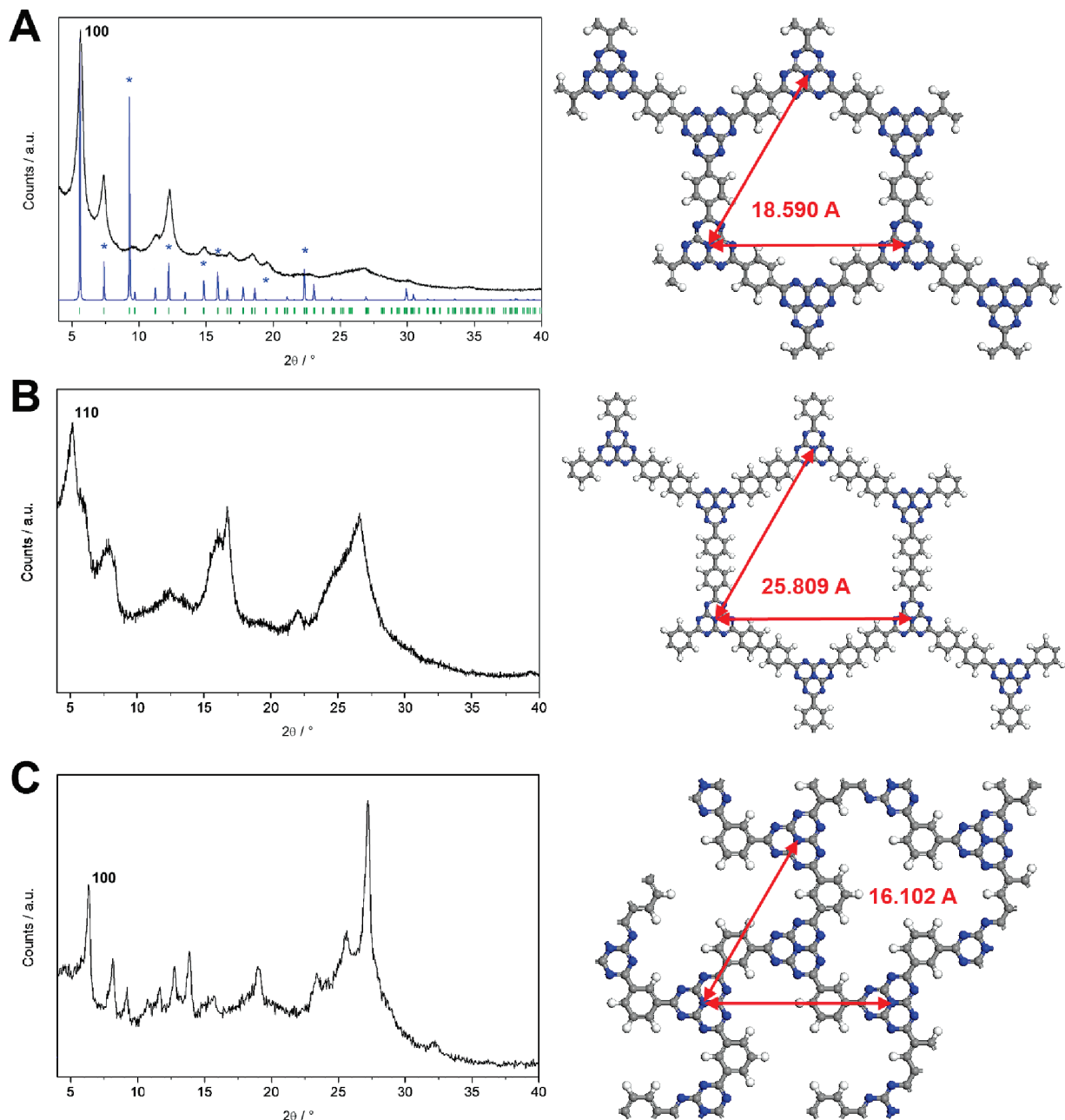


Figure 4. Observed (black) and calculated (blue) PXRD profiles with Bragg peak positions (green) of (A) HBF-1, (B) HBF-2, and (C) HBF-3. Calculated reflections with a mixed-in l -component are marked (* in blue). Underlying atomic connectivity pattern with carbon, nitrogen, and hydrogen is represented as gray, blue, and white spheres, respectively.

26–27° in terms of 2θ for HBF-1, corresponds to approximately 3.3 Å—an interplanar stacking distance of the order of magnitude of graphite (3.35 Å).

Also HBF-2 and HBF-3 show crystallinity in the XRD pattern, while especially the broad peaks in HBF-2 point to a rather ill-defined crystal structure. Unfortunately, there is no chemically intuitive, obvious pattern and no clear hint from unit-cell indexing (see Supporting Information) as to how the individual sheet should be related. This is especially true for HBF-2 for which the linking biphenyl group will experience steric repulsion, and as a result most likely will twist out of plane. Thus, crystallization of the HBF-2 framework to long-range ordered crystals is inherently difficult. It can be speculated whether a singular monodomain of long-range order in the c -direction can be achieved at all for systems with a very weak interplanar correlation and a near-infinite number of possibilities of how to relate

from one sheet to the next, varying not only by translation but potentially also by torsion. It is also a distinct possibility that several domains of varying degrees of interplanar order are present at any one-time for each framework, rendering them “phase impure” with respect to the c -direction of each unit-cell. Nonetheless, the near-equivalence in $(hk0)$ reflections for each system and a chemically reasonable occupation of any singular sheet supports the assertion that the synthesized HBF materials are sufficiently well described by the modeled structures (cf. Figure 4 and Supporting Information). Assuming the calculated unit-cell parameters in a - and b -direction given above and in the Supporting Information a layer-to-layer packing distance of approximately 3.3 Å, the theoretical densities of HBF-1, HBF-2, and HBF-3 are 0.803, 0.592, and 1.055 g cm⁻³, respectively. Volumetric density measurements for the dried frameworks gave values of 0.984, 0.777, and 1.033, which further corroborates the

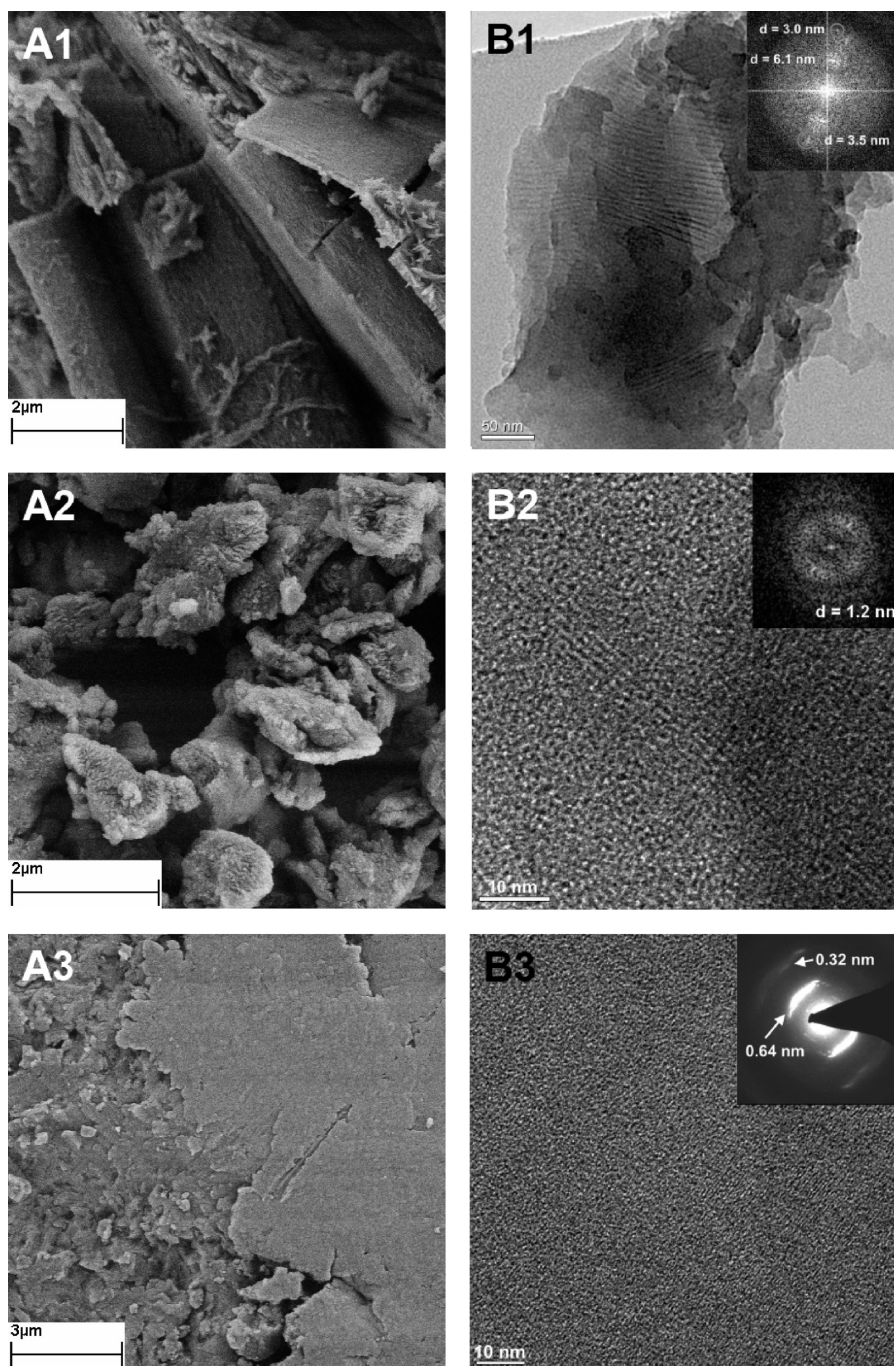


Figure 5. Representative SEM images of HBF-1, HBF-2, and HBF-3 (A1, A2, and A3, respectively) and TEM images, showing (B1) TEM image showing a Moiré pattern and (B1, inset) the Fourier transform as observed for HBF-1, (B2) TEM image and (B2, inset) the Fourier transform showing a packing repeat of layers as observed for HBF-2, and (B3) TEM image and (B3, inset) the Fourier transform showing a packing repeat of layers as observed for HBF-3.

structural model and the fact that the described pores are essentially empty.

Scanning electron microscopy (SEM and transmission electron microscopy (TEM) reveal further indicators of the atomic, molecular and supramolecular order of the frameworks. The selection of images of HBF-1 in Figure 5 shows lamellar features (A1 and B1), indicative of the interplanar correlation. However, the sheer order of magnitude of the distances between ordered repeats is in the range of several nanometers, i.e., an n -fold of the modeled unit-cell dimensions in each direction. In order to discard any artifacts produced by camera or substrate, pictures were taken at different camera lengths and magnifications and with samples lying directly on carbon support as well as off it

(cf. Supporting Information). In each case the nanometer-sized superstructures remained visible, indicating, that they are interference (Moiré) patterns of real, atomic (or molecular) highly ordered structures. Torsional distortion of layers which can freely rotate with respect to one-another—as mentioned previously in the structural discussion based on PXRD data—is a likely cause of Moiré interference and was reported previously for different systems.^{32–34} Parts B2 and B3 of Figure 5 show the representative TEM images of HBF-2 and HBF-3, respectively. Although the outer shape of the aggregates in the SEM overviews (cf. Figure 5, parts A2 and A3) does not seem to reveal any sharp edges known for crystalline systems, higher resolved TEM images indicate an ordering on molecular length scale with parallel “fringes”

separated by 1.2 nm (approximately four layers) for HBF-2 (Figure 5, part B2) and 0.64 nm (approximately two layers) for HBF-3 (Figure 5, part B3).

The architectural stability and porosity of HBF-1, HBF-2, and HBF-3 was initially studied by measuring nitrogen adsorption, however the results in the order of magnitude of approximately $30 \text{ m}^2 \text{ g}^{-1}$ external surface area indicated that the pores are essentially not accessible from the outside. This is a standard problem of organic frameworks where smaller amounts of organic side products or monomers can easily block a majority of the channel system in a dynamic fashion. The fact that the pores are in principle open to the outside can be deduced from the fact that we were able to remove all but tiny traces of salt by simple washing with water.

Subsequently, a water adsorption study was performed on the guest-free materials, and commercially available graphite and clay (kaolinite) were chosen as reference systems. Samples of "as-synthesized" HBF-1, HBF-2, HBF-3, graphite and clay were evacuated at 10^{-5} Torr vacuum pressure and heated to 180°C for 12 h to remove solvents. The samples were then used for measurement of the isotherm from 0 to 1 bar water vapor pressure, which shows gradual uptake at p/p_0 from 0.05 to 0.6, and some features of accessible micropores for HBF-3 (cf. Supporting Information). The slow rise in the isotherm occurring at higher pressures is due to the existence of a small population of external mesopores between the crystallites; this feature is not uncommon for particles with platelet morphology.³⁵ Unfortunately, the Brunauer–Emmett–Teller (BET) model cannot be reliably applied to water adsorption, so no apparent surface area can be given. A powder X-ray diffraction experiment was performed to monitor the effect of water on the dried and evacuated frameworks. Although it should be noted, that the general intensity of the all reflections is attenuated due to low contrast between the constituent light atoms (C, N, H) and water, the general finding is that the uptake of water is accompanied by a broadening of the peak at 26 to 27° (in terms of 2θ), which was identified as an indicator of layer-to-layer ordering, while the principal ($hk0$) reflection persist (cf. Supporting Information). This suggests that the water uptake is accompanied by swelling and disordering of individual layers of the framework. Overall, this study shows that the materials HBF-1, HBF-2, and HBF-3 behave analogous to previously known layered materials (especially clays) with respect to water uptake, and that these laterally continuous polymers can principally be separated into mono- or at least oligo-layers by physical exfoliation.

Conclusion

In this manuscript, a simple and convenient pathway toward a family of regular, two-dimensional polymer structures based on heptazine units, HBF-1, HBF-2, and HBF-3, was presented. Furthermore, and foremost, a new way of linking organic building blocks into well-ordered aggregates purely by strong covalent bonds in a manner which overcomes the thermodynamic and kinetic limitations known from crystallization and condensation processes is employed. The procedure to prepare the triazine- and carbonitrile-functionalized precursors for thermally induced autocondensation is likely to be easily adaptable to a multitude of molecules of 2D or 3D symmetry. All three synthesized frameworks and other possible heptazine-based structures are intellectually appealing, and they hold exiting prospects as lightweight materials optimized for low k -dielectrics, thermal insulation and phonon damping. Further work has also to address the question of pore opening by etching or purification processes.

Acknowledgment. This work was funded by the Project House "ENERCHEM" of the Max Planck Society. We would like to thank Sören Selve from the TU Berlin for his aid and patience with TEM imaging and Regina Rothe from the Max Planck Institute of Colloids and Interface for the water adsorption measurements.

Supporting Information Available: Figures showing NMR spectra, FTIR spectra, TGA plots, TEM images, DSC plots, and PXRD analysis, and a table of elemental microanalysis data. This material is available free of charge via the Internet at <http://pubs.acs.org>.

References and Notes

- Geim, A. K.; Novoselov, K. S. *Nat. Mater.* **2007**, *6* (3), 183–191.
- Yaghi, O. M.; O'Keeffe, M.; Ockwig, N. W.; Chae, H. K.; Eddaoudi, M.; Kim, J. *Nature* **2003**, *423* (6941), 705–714.
- El-Kaderi, H. M.; Hunt, J. R.; Mendoza-Cortes, J. L.; Cote, A. P.; Taylor, R. E.; O'Keeffe, M.; Yaghi, O. M. *Science* **2007**, *316* (5822), 268–272.
- Bojdys, M. J.; Muller, J. O.; Antonietti, M.; Thomas, A. *Chem.—Eur. J.* **2008**, *14*, 8177–8182.
- Kuhn, P.; Antonietti, M.; Thomas, A. *Angew. Chem., Int. Ed.* **2008**, *47*, 3450–3453.
- Kuhn, P.; Forget, A.; Su, D. S.; Thomas, A.; Antonietti, M. *J. Am. Chem. Soc.* **2008**, *130*, 13331–13337.
- Blake, A. J.; Champness, N. R.; Hubberstey, P.; Li, W. S.; Withersby, M. A.; Schroder, M. *Coord. Chem. Rev.* **1999**, *183*, 117–138.
- Colvin, V. L.; Goldstein, A. N.; Alivisatos, A. P. *J. Am. Chem. Soc.* **1992**, *114*, 5221–5230.
- Decher, G. *Science* **1997**, *277* (5330), 1232–1237.
- Kim, Y. H. *J. Polym. Sci., Polym. Chem.* **1998**, *36*, 1685–1698.
- Voit, B. *J. Polym. Sci., Part A: Polym. Chem.* **2000**, *38*, 2505–2525.
- Sakamoto, J.; van Heijst, J.; Lukin, O.; Schluter, A. D. *Angew. Chem., Int. Ed.* **2009**, *48*, 1030–1069.
- Yaghi, O. M.; Li, H. L.; Davis, C.; Richardson, D.; Groy, T. L. *Acc. Chem. Res.* **1998**, *31*, 474–484.
- Liebig, J. v. *Ann. Pharm.* **1834**, 10.
- Hosmane, R. S.; Rossman, M. A.; Leonard, N. J. *J. Am. Chem. Soc.* **1982**, *104*, 5497–5499.
- May, H. J. *Appl. Chem.* **1959**, *9*, 340–344.
- Lotsch, B. V.; Schnick, W. *Chem.—Eur. J.* **2007**, *13*, 4956–4968.
- Kanatzidis, M. G.; Park, Y. *Chem. Mater.* **1990**, *2*, 99–101.
- Solomons, C.; Goodkin, J.; Gardner, H. J.; Janz, G. J. *J. Phys. Chem.* **1958**, *62*, 248–250.
- Laitinen, H. A.; Tischer, R. P.; Roe, D. K. *J. Electrochem. Soc.* **1960**, *107*, 546–555.
- Cassayre, L.; Serp, J.; Soucek, P.; Malmbeck, R.; Rebizant, J.; Glatz, J. P. *Electrochim. Acta* **2007**, *52*, 7432–7437.
- Sundermeyer, W. *Angew. Chem.* **1965**, *77*, 241–258.
- Sundermeyer, W. *Chem. uns. Zeit* **1967**, *1*, 150–157.
- Verbeek, W.; Sundermeyer, W. *Angew. Chem.* **1967**, *79*, 860–861.
- Sundermeyer, W. *Z. Anorg. Allgem. Chem.* **1961**, *310*, 50–52.
- Bojdys, M. J.; Jeromenok, J.; Thomas, A.; Antonietti, M. *Adv. Mater.* **2010**, *22*, 2202–2205.
- Jurgens, B.; Irran, E.; Senker, J.; Kroll, P.; Muller, H.; Schnick, W. *J. Am. Chem. Soc.* **2003**, *125*, 10288–10300.
- Miller, D. R.; Swenson, D. C.; Gillan, E. G. *J. Am. Chem. Soc.* **2004**, *126*, 5372–5373.
- El-Gamel, N. E. A.; Seyfarth, L.; Wagler, J.; Ehrenberg, H.; Schwarz, M.; Senker, J.; Kroke, E. *Chem.—Eur. J.* **2007**, *13*, 1158–1173.
- Holst, J. R.; Gillan, E. G. *J. Am. Chem. Soc.* **2008**, *130*, 7373–7379.
- Cote, A. P.; Benin, A. I.; Ockwig, N. W.; O'Keeffe, M.; Matzger, A. J.; Yaghi, O. M. *Science* **2005**, *310* (5751), 1166–1170.
- Bassett, G. A.; Menter, J. W.; Pashley, D. W. *Proc. R. Soc. London, Ser. a: Math. Phys. Sci.* **1958**, *246* (1246), 345.
- Dawson, I. M.; Follett, E. A. C. *Proc. R. Soc. London, Ser. a: Math. Phys. Sci.* **1959**, *253* (1274), 390.
- Gevers, R.; Delavignette, P.; Blank, H.; Amelinckx, S. *Phys. Status Solidi* **1964**, *4* (2), 383–410.
- Rouquerol, F.; Rouquerol, J.; Sing, K. *Adsorption by Powders and Porous Solids*; Academic Press: London, 2002.